Proceedings of the European Conference "Physics of Magnetism" (PM'08), Poznań 2008

Ru_3Sn_7: Phonon Reference for Superconducting Mo_3Sb_7

V.H. Tran and W. Miiller

W. Trzebiatowski Institute of Low Temperature and Structure Research

Polish Academy of Sciences, P.O. Box 1410, 50-950 Wrocław, Poland

In order to search for phonon reference for dimer-gapped superconducting Mo_3Sb_7, measurements of specific heat ($C_p(T)$) and electrical resistivity ($\rho(T)$) of Ru_3Sn_7 were performed in the temperature range 2–300 K. The phonon part of $C_p(T)$ and $\rho(T)$ of Ru_3Sn_7 can satisfactorily be explained describing the spectrum with one Einstein and two Debye modes. We found $\Theta_E \approx 100$ K, $\Theta_{D1} \approx 185$ K and $\Theta_{D2} \approx 298$ K. The magnetic specific heat of Mo_3Sb_7 exhibits a sharp maximum at $T^* = 50$ K, below which follows a gap function. Magnetic resistivity increases as $-\ln T$ with decreasing temperature and shows maximum at T^*.

PACS numbers: 65.40.−b, 72.15.Eb, 74.25.Kc, 74.25.Bt, 72.15.Qm

1. Introduction

Several years ago, Bukowski and co-workers reported the superconductivity in an intermetallic Mo_3Sb_7 [1]. Although with rather low T_C of 2.1 K the material is interesting in many aspects. According to the recent report, Mo_3Sb_7 is a spin fluctuation superconductor [2]. Very recently, we have measured low-temperature specific heat on a polycrystalline sample and found a large Sommerfeld coefficient, which has been attributed to a narrow Mo 4*d* band pinned at the Fermi level. Furthermore, the electronic specific heat and muon spin-rotation in the superconducting state have been ascribed to the presence of two BCS-like gaps with $2\Delta_1 = 4.0k_BT_c$ and $2\Delta_2 = 2.5k_BT_c$ and $2\Delta_1 = 4.54k_BT_c$ and $2\Delta_2 = 2.73k_BT_c$, respectively [3]. Interestingly, in addition to the superconductivity transition, Mo_3Sb_7 exhibits a pronounced maximum around 50 K in the specific heat, for which the behavior may be interpreted as the opening of a dimerization gap [4]. Thus, the feature resembles very much a complex phase diagram found in high-temperature superconductors [5]. In this contribution, we report on measurements of specific heat and electrical resistivity for Ru_3Sn_7 aiming to search for phonon reference for superconducting Mo_3Sb_7. Previously, we used $Ir_3Ga_3Ge_4$ as a phonon reference for Mo_3Sb_7 [4]. However, owing to the closer molar mass and binary stoichiometric, Ru_3Sn_7 seems to be a better candidate. The obatined data on Ru_3Sn_7 in this work will be used to analyze the magnetic contribution to the specific heat and electrical resistivity of Mo_3Sb_7 [3, 7]. One may recall that the electrical resistivity and magnetization of Ru_3Sn_7 were measured by Chakoumakos and Mandrus [6]. The compound was reported to be metallic and diamagnetic above 150 K.

2. Experimental details

Single crystals of Ru_3Sn_7 were grown using a tin-flux method. A mixture of good quality elements Ru (purity at. 99.99%) and Sn (at. 99.999%) with the atomic ratio Ru:Sn = 1:10 was placed in an alumina crucible and sealed in an evacuated quartz ampoule. The ampoule was heated with a heating rate of 15°C/h up to 1050°C and kept at this temperature for 4 h, followed by cooling down to 400°C with a step of 2°C/h. Then the ampoule was cooled down to room temperature. The excess of Sn was removed by etching in HCl. The obtained single crystals with typical dimension $0.2 \times 0.2 \times 0.5$ mm^3 were examined by a scanning electron microscope Phillips 515 and an energy dispersive X-ray spectrometer PV9800. The room temperature X-ray powder diffraction data indicated the sample to be single phase crystallizing in the cubic Ir_3Ge_7-type structure. Lattice parameter determined from least-squares refinements was $a = 0.9374$ nm, in good agreement with previously reported [6]. The specific heat C_p measurement was performed on pelleted pieces using the thermal relaxation method and the electrical resistivity ρ was measured using a conventional four-probe ac-technique with a current of 10 mA. Both measurements were utilized on Quantum Design PPMS device in the temperature range 2–300 K.

3. Results

The specific heat of Ru_3Sn_7 is plotted in Fig. 1 in the form of C_p/T vs. T. As expected, no magnetic order could be detected down to 2 K and there is a dominant contribution of lattice vibrations. At 200 K, C_p reaches a value of about 90% of the Dulong–Petit equipartition, indicating that the Debye temperature is of the same order of magnitude of room temperature. In general, the lattice vibrations are described by acoustic and/or optical phonons. For a compound having n atoms per unit cell, one expects 3 acoustical and $3n - 3$ optical modes. The acoustical modes are represented as the Debye oscillators, which contribute to the total specific heat as

$$C_{\mathrm{ph,D}}(T) = 9Rn_{\mathrm{D}}(T/\Theta_{\mathrm{D}})^3 \int_0^{\Theta_{\mathrm{D}}/T} \frac{x^4 \exp(x)}{[\exp(x)-1]^2}\mathrm{d}x,$$

while the optical modes are presented as

$$C_{\mathrm{ph,E}}(T) = 3Rn_{\mathrm{E}} \frac{(\Theta_{\mathrm{E}}/T)^2 \exp(\Theta_{\mathrm{E}}/T)}{[\exp(\Theta_{\mathrm{E}}/T)-1]^2}\mathrm{d}x,$$

where R is the gas constant, Θ_{D}, Θ_{E}, n_{D} and n_{E} are the Debye temperature, the Einstein temperature, number of the Debye oscillators and number of the Einstein oscillators, respectively [8]. For Ru_3Sn_7 the presence of the optical phonons is evidenced by the plot C_p/T^3 vs. T shown in the inset of Fig. 1. Clearly, below 150 K an upward deviation from the T^3-Debye law is observed and at about 20 K there appears a maximum, which roughly corresponds to the Einstein temperature of $\Theta_{\mathrm{E}} = 100$ K. It turns out that to get a satisfactory description of the phonon specific heat data of Ru_3Sn_7 one uses one optical mode and two acoustic modes with $\Theta_{\mathrm{E}} = 100(2)$ K, $\Theta_{\mathrm{D1}} = 185(3)$ K and $\Theta_{\mathrm{D2}} = 298(5)$ K, and $n_{\mathrm{E}} = 1(0.2)$, $n_{\mathrm{D1}} = 1.5(0.2)$ and $n_{\mathrm{D2}} = 7.5(0.3)$. In the fit of the data we also took into account the electronic heat capacity with the coefficient of 6.5 mJ $\mathrm{mol}_{\mathrm{Ru}}^{-1}$ K^{-2}. The solid line in Fig. 1 presents the result of the best fit.

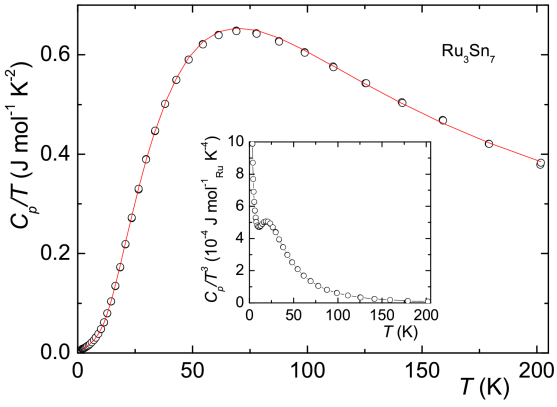

Fig. 1. Temperature dependence of the specific heat of Ru_3Sn_7 divided by temperature. The solid line is a fit with one Einstein and two Debye modes plus electronic specific heat. The inset shows the ratio C_p/T^3 as a function of temperature aiming to illustrate the presence of the optical phonons.

Assuming the validity of the relation $(\Theta_{\mathrm{D}}, \Theta_{\mathrm{E}}) \sim \sqrt{1/m}$, m = molar mass, we have taken into consideration the mass effect, and we plot phonon specific heat C_{ph} of Mo_3Sb_7 in Fig. 2 as a solid line. If phonon spectra in Ru_3Sn_7 and Mo_3Sb_7 were similar to one another, one determines magnetic contribution to specific heat of Mo_3Sb_7 as the difference $C_{\mathrm{mag}} = C_{p,\mathrm{Mo3Sb7}} - C_{\mathrm{ph}}$. The resulting magnetic specific heat, shown in the inset of Fig. 2, exhibits clear phase transition at $T^* = 50(1)$ K. The nature of this transition has already been discussed in Ref. [4] as due to dimerization of the Mo atoms. For low-temperature data of C_{mag} we were able to fit to formula $C_{\mathrm{mag}} \sim (\Delta/k_{\mathrm{B}}T)^2 \exp(-\Delta/k_{\mathrm{B}}T)$ with dimer gap Δ/k_{B} of 195 K. We note that this value is substantially larger than that previously determined, i.e., of 113 K [4].

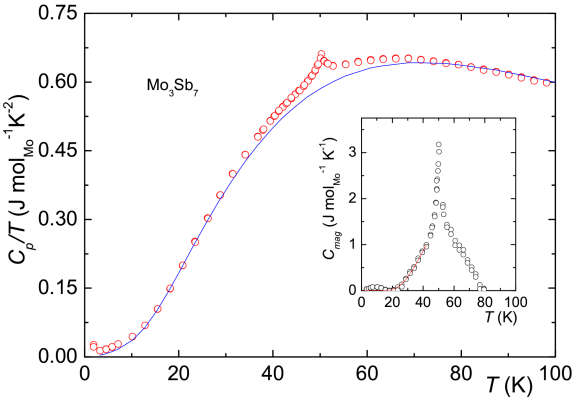

Fig. 2. Temperature dependence of the specific heat of Mo_3Sb_7 [4] and phonon contribution deduced from the specific heat of Ru_3Sn_7 shown as solid line. Inset: the magnetic specific heat of Mo_3Sb_7 and theoretical line of specific heat for isolated dimers (solid line).

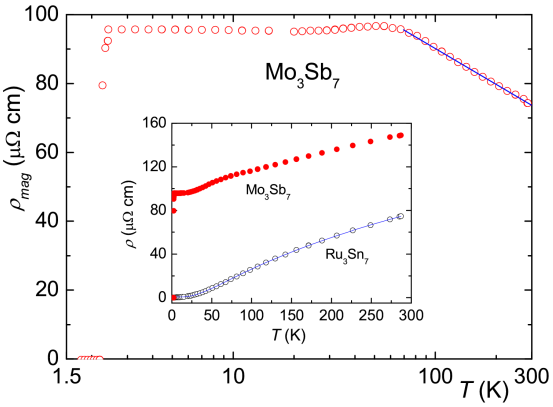

Fig. 3. Temperature dependence of the magnetic resistivity of Mo_3Sb_7. The solid line demonstrates a $-\ln T$ dependence of ρ_{mag}. The inset shows the resistivity of Mo_3Sb_7 [4] and of Ru_3Sn_7. The solid line is a fit to a parallel resistor model.

The temperature dependence of electrical resistivity of Mo_3Sb_7 [4] and of Ru_3Sn_7 is depicted in the inset of Fig. 3. The resistivity of Ru_3Sn_7 displays a standard metal-like behavior thus our data essentially agree with those reported by Chakoumakos and Mandrus [6]. To analyze our data we used the parallel resistor model [9], which was successfully applied for A15-type superconductors. In this model, the resistivity is given by the relation

$$\frac{1}{\rho(T)} = \frac{1}{\rho_{\mathrm{ideal}}(T)} + \frac{1}{\rho_{\mathrm{sat}}}, \qquad (1)$$

where ρ_{sat} is the saturation resistivity and it is independent of temperature, while $\rho_{\mathrm{ideal}}(T)$ is the ideal resistiv-

ity, i.e. that as would be expected if there were no limiting value of the mean free path respect to the interatomic distance. The temperature dependence of $\rho_{\rm ideal}(T)$ is the sum of the residual resistivity ρ_0 and the resistivity due to phonon-assisted electron scattering. In Ru_3Sn_7 the latter contribution arises from the scattering of electrons with acoustic phonons and with optical phonons. Thus, the ideal resistivity is given by the following expression: $\rho_{\rm ideal}(T) = \rho_0 + d_1 F(\Theta_{\rm D1}/T) + d_2 F(\Theta_{\rm D2}/T) + e F(\Theta_{\rm E}/T)$, where d_1, d_2 and e are numerical constants, $F(\Theta_{\rm D}/T)$ is the Bloch–Grüneisen function for acoustic phonons

$$F(\Theta_{\rm D}/T) = \left(\frac{T}{\Theta_{\rm D}}\right)^5 \int_0^{\Theta_{\rm D}/T} \frac{x^5}{[1-\exp(-x)][\exp(x)-1]}{\rm d}x$$

and $F(\Theta_{\rm E}/T)$ is a similar expression for the resistivity of optical phonons

$$F(\Theta_{\rm E}/T) = \frac{\Theta_{\rm E}}{T} \frac{1}{[1-\exp(-\Theta_{\rm E}/T)][\exp(\Theta_{\rm E}/T)-1]}.$$

As can be seen from the inset of Fig. 3, the overall data of Ru_3Sn_7 could be well fitted to Eq. (1). From the fit we get the values of ρ_0, d_1, d_2, e and $\rho_{\rm sat}$ to be 1, 0.87, 0.68, 1.37 and 220 $\mu\Omega$ cm, respectively. It is interesting to see that the magnetic resistivity of Mo_3Sb_7, which was approximately estimated as the difference $\rho_{\rm mag}(T) = \rho_{\rm Mo3Sb7}(T) - \rho_{\rm Ru3Sn7}(T) - \rho_0$. Apparently, $\rho_{\rm mag}(T)$ exhibits a maximum at the same temperature as the $C_{\rm mag}$ does. In the temperature range 70–300 K, one recognizes $\rho_{\rm mag}(T) \sim -\ln T$ dependence. Tentatively, one suspects the presence of the Kondo effect, where due to scattering of the conduction electrons the magnetic moments of the localized Mo ions become screened by the spins of these electrons. The Kondo effect thus facilitates an increase in the resistivity in a form of $-\ln T$ below the Kondo temperature. The solid line in Fig. 3 corroborates a $-\ln T$ dependence. However, other mechanisms such as weak localization cannot be excluded, and therefore, should be taken into consideration.

4. Conclusions

We have measured specific heat and electrical resistivity for Ru_3Sn_7 in the temperature range 2–300 K. We found evidence for low-lying optical mode, which is most probably due to lattice vibrations of the Ru atoms. The temperature dependence of the phonon part of $C_p(T)$ and $\rho(T)$ can be described by one Einstein ($\Theta_{\rm E} \approx 100$ K) and two Debye temperatures ($\Theta_{\rm D1} \approx 185$ K and $\Theta_{\rm D1} \approx 298$ K). We have determined magnetic contributions to specific heat and resistivity, that originate from the interactions between Mo–Mo atoms. The phase transition at $T^* = 50$ K, where dimerization of Mo atoms sets in, shows up distinct anomaly in $C_{\rm mag}(T)$ and $\rho_{\rm mag}$. Below T^*, $C_{\rm mag}$ follows a gap function, while $\rho_{\rm mag}$ exhibits a $-\ln T$ dependence in the temperature range 70–300 K. We suggest that Ru_3Sn_7 may be a suitable candidate for phonon reference for superconducting Mo_3Sb_7.

Acknowledgments

The authors would like to thank the Ministry of Science and Higher Education in Poland for financial support within the grant No. N202 082 31/0449.

References

[1] Z. Bukowski, D. Badurski, J. Stępień-Damm, R. Troć, *Solid State Commun.* **123**, 283 (2002).

[2] C. Candolfi, B. Lenoir, A. Dauscher, C. Bellouard, J. Hejtmanek, E. Santava, J. Tobola, *Phys. Rev. Lett.* **99**, 037006 (2007).

[3] V.H. Tran, W. Miiller, Z. Bukowski, ArXiv:0803.2948; *Acta Mater.* **56**, 5694 (2004); V.H. Tran, A.D. Hillier, D.T. Adroja, Z. Bukowski, *Phys. Rev. B* **78**, 172505 (2008).

[4] V.H. Tran, W. Miiller, Z. Bukowski, *Phys. Rev. Lett.* **100**, 137004 (2008).

[5] B. Batlogg, C. Varma, *Physics World* **13**, 33 (2000).

[6] B.C. Chakoumakos, D. Mandrus, *J. Alloys Comp.* **281**, 157 (1998).

[7] V.H. Tran, Z. Bukowski, *Acta Phys. Pol. A* **114**, 73 (2008).

[8] E.S.R. Gopal, *Specific Heats at Low Temperatures*, Plenum, New York 1996.

[9] H. Wiesmann, M. Gurvitch, H. Lutz, A.K. Ghosh, B. Schwarz, M. Strongin, P.B. Allen, J.W. Halley, *Phys. Rev. Lett.* **38**, 782 (1977).